FRISPEE: FRI-Based Single Image Super-Resolution with Deep Recursive Residual Network

Renke Wang*, Jun-Jie Huang†, Pier Luigi Dragotti*
*Imperial College London
†National University of Defense Technology
email: renke.wang19@imperial.ac.uk, jjhuang@nudt.edu.cn, p.dragotti@imperial.ac.uk

***Abstract*—In this paper, we propose a novel single image super-resolution algorithm that integrates a model-based approach with self-learning deep networks. The proposed method can be adapted to low-resolution (LR) images obtained with real acquisition devices where the point spread function is Gaussian-like. By modelling natural image lines as piece-wise smooth functions and approximating the blurring kernel with B-splines, an intermediate high-resolution (HR) image can be first obtained based on Finite Rate of Innovation theory. A self-supervised deep recursive residual network is then applied to further enhance the reconstruction quality. From the simulation results, our algorithm outperforms other self-learning algorithms and achieves state-of-the-art performance.**

***Index Terms*—single image super-resolution, finite rate of innovation, self-learning, wavelet theory**

I. Introduction

Single image super-resolution (SISR) is a challenging task where the aim is to recover a sharp high-resolution (HR) image from its blurred low-resolution (LR) version. In recent years, supervised deep convolutional neural networks (DCNN) [1]–[10] have been widely applied to SISR and they have demonstrated prominent superiority over non-deep methods [11]–[19]. However, it is widely acknowledged that the performance of such methods would deteriorate drastically when testing data mismatch with the training degradation model [20]. Several recent works have considered more diverse degradation settings using generative adversarial networks [21]–[23] and Transformers [24], but they require huge labelled external datasets and intensive training time and resources. Besides the above mentioned supervised methods, Schoher *et al.* [25], [26] have proposed to use a self-supervised CNN to exploit internal recurrence of information within a single LR image, however, its resultant images are shown to lack high frequency details.

We notice that during an acquisition process, various sources may contribute to the blurring of a digital image, for example, lens blur, motion and limited numbers of sensors [27]. Therefore, the overall point spread function (PSF) introduced by a digital acquisition device can often be characterized by a 2D Gaussian kernel. Given this observation, we propose a novel method that combines self-learning with a model-based approach which enables us to exploit the properties of the blurring kernels. We note that the image formation process is similar to the traditional sampling scheme where the analogue signal (natural scene) is low-pass filtered (lens blurring effect) and sampled (sensor grid) [15]. To exploit this analogy, we propose to model scan lines of natural images as piece-wise smooth functions composed of a globally smooth signal, and a piece-wise polynomial signal as shown in Fig. 1. Moreover, we approximate Gaussian blurring kernels with B-splines [29], which are able to provide multi-resolution representations for our assumed signal model.

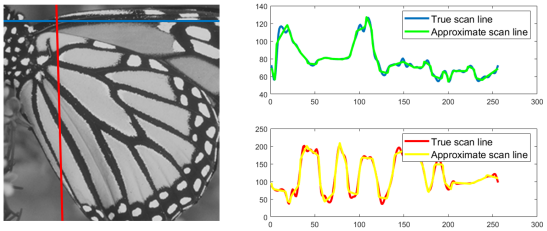

Fig. 1. Scan-lines of natural images are approximated as piecewise smooth functions.

By doing so, the LR images are modeled as noisy samples of piecewise smooth signals obtained with B-spline kernels. Finite Rate of Innovation (FRI) theory has provided a model-based approach to reconstruct the high-resolution piecewise polynomial signal from the noisy low-resolution samples, and thus, a reliable way to map a given low-resolution signal to its higher-resolution version [28]. This model-based super-resolution will enable the retrieval of high-pass details from a single LR image. However, due to the imprecision of the piecewise smooth assumption of the natural image and kernel approximation, the FRI-upsampled images may contain artefacts. Therefore, we further exploit the power of deep networks to refine the FRI-upsampled image in a self-supervised manner. We train an image-specific deep network with patch pairs extracted solely from the FRI-upsampled and original LR images. The network is implicitly adapted to the specific down-sampling kernel. The overall algorithm is in the form of a two-stage pyramid structure which integrates the FRI-based upsampling and deep networks and enables us to exploit cross-scale internal recurrence of information at different scales [30]. The contribution of this paper is three-fold:

- We introduce a novel SISR algorithm that integrates the use

of an FRI-based approach with a properly designed deep network for self-learning.
- By leveraging the ability of splines to approximate realistic PSF, the proposed method is able to adapt well to a broad category of sampling kernel.
- The proposed method achieves state-of-the-art performance among self-learning SISR algorithms.

The rest of the paper is organised as follows: In Section II, we briefly discuss some related works. In Section III, we introduce our proposed FRISPEE algorithm for single image super-resolution. We show simulation results and further analyse the method in Section IV. We then conclude in Section V.

II. Related work

A. FRI-Based Image Upsampling

FRESH [15] is the pioneering work to model image scan lines as piecewise smooth signals and apply FRI-based method to super resolve a LR image. However, the downscaling kernel is restricted to scaling functions. Moreover, resolution refinement is achieved by applying a linear transformation learned from neighbor patches. Deng *et al.* [39] further combined FRESH with a local regression learning approach.

B. Zero-Shot Super-Resolution

ZSSR [25] is a self-supervised CNN architecture where the network is trained from LR-HR pairs generated from a single image. It is able to learn internal information to given image statistics. MZSR [40] further incorporates meta transfer learning which effectively learns an initial weight for fast adaption in the zero-shot unsupervised setting.

III. Proposed method

The overall FRISPEE algorithm is composed of a model-based approach based on FRI theory and a self-learning deep recursive residual network (DRRN) for further refinement. In Section III-A, we explain the FRI model-based image upsampling, in particular, the approximation of Gaussian blurring kernels with B-splines. We then introduce in Section III-B the two-stage pyramid structure of FRISPEE. In Section III-C, the architecture and implementation details of the self-supervised DRRN is introduced, which enhances the super-resolved quality of the output of the model-based approach. We consider bivariate Gaussian blurring kernels k_s with arbitrary variances along the horizontal and vertical axes.

A. Approximating 2D Gaussian kernel with B-splines

The basic idea behind approximating Gaussian PSF with B-splines is to apply the fast and efficient FRI-upsampling to images, such that high-pass details can be estimated from the set of FRI images (stacks of high-resolution piecewise polynomials). This provides a strong and universal baseline for image upsampling in the presence of Gaussian-like PSF.

We propose to use B-splines to approximate the Gaussian PSF for the following reasons: first, B-splines have a similar shape as the Gaussian pulse [37], [38]; Second, they possess the polynomial reproduction property, which suits our modelling of lines of images as piecewise polynomials with noise. Moreover, B-spline wavelets and scaling functions are able to provide a multi-resolution representation of a signal at different scales.

We denote the n^{th} order B-spline with β_n, which is obtained as the $(n+1)^{th}$ fold convolution of the box function β_0 and has a support of $n+1$. The 2D FRI image upsampling algorithm [15] synthesizes the recovered highpass detail coefficients with the LR image using two-branch filter bank reconstruction, which means the support of the chosen B-spline function is related to the level of filter bank [32]. Here we mainly consider up-scaling factors of 2 and 4, which correspond to 1 and 2-level filter bank.

The bivariate Gaussian kernel is modeled as the Kronecker product of two B-splines each along horizontal and vertical directions. The chosen filters β_n^h, β_n^v are such that after iterating on the low-pass branch in a 1 or 2-level filter bank, their final kernel size is the closest to the effective Gaussian kernel size. We perform the estimation of the effective kernel size on the central row and column of the kernel. Samples on these lines are normalized, and set to zero if their absolute values are smaller than $\epsilon = 10^{-2}$. The chosen n-th order B-spline functions will serve as the low-pass decomposition filters (LoD) in the biorthogonal filter bank. The other filters can then be determined by resorting to standard expressions [33]. Given two sets of filter banks each along horizontal and vertical directions, the 2D FRI upsampling is then achieved by applying the 1D FRI upsampling on each image lines along these directions and retrieve image detail coefficients through 2D wavelet decomposition (please refer to [15] for more details).

B. The FRISPEE algorithm

Given the super-resolved FRI image, we train a DRRN to correct the artefacts in the FRI upsampled image from another upsampled image, which may not contain as many highpass details, but have smoother textures. To do so, we leverage the power of cross scale recurrence of information within a single image, and train the network from pairs of images obtained from its downscaled version. We notice that there is a clear balance between maintaining as many highpass details as possible and removing the artefacts. Therefore, we introduce a two-stage algorithm as depicted in Fig. 2, in which the ground-truth (GT) image at the first stage is obtained using bicubic interpolation, and at the second stage it is replaced with the output of the first stage. Now we will provide a detailed explanation on the FRISPEE algorithm.

For simplicity, we denote with I_0 the LR image and its upsampled version by factor 2^k at i^{th} stage with $I_{i,k}$, where $i = 1, 2$ and $k \in \mathbb{R}$. For a desired resolution level $2^K, K \in \mathbb{Z}^+$, the training pairs are set to a lower resolution level 2^{K-m} with $m \in (0, 1)$. Images obtained using FRI upsampling are denoted with superscript FRI. At the first stage as shown in Fig. 2 (a), step 1, the GT image $I_{1,K-m}$ is obtained by

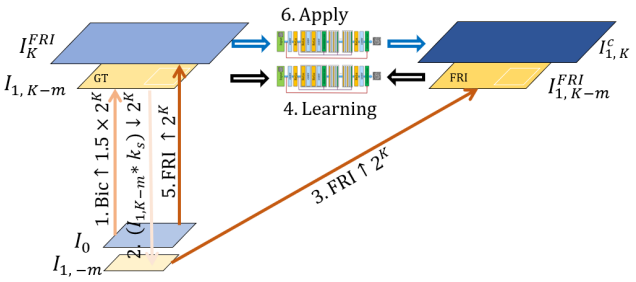

(a) The first stage of FRISPEE algorithm. The training GT image is obtained using bicubic interpolation at the resolution level $1.5 \times 2^{K-1}$.

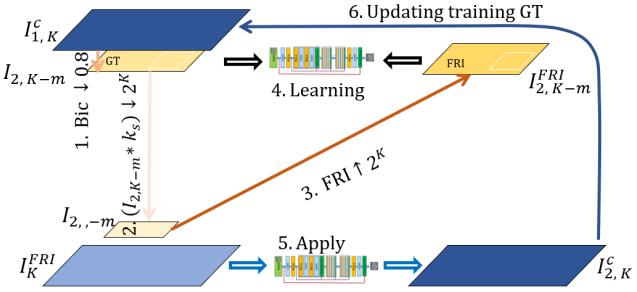

(b) The second stage of FRISPEE algorithm. The training GT image is updated using the output of the first stage at the resolution level $1.6 \times 2^{K-1}$.

Fig. 2. The scheme of the two-stage FRISPEE algorithm.

up-scaling the LR image I_0 with a factor $1.5 \times 2^{K-1}$ using bicubic interpolation, in this case $m = -\log_2 0.75$. In step 2, the downscaled LR image $I_{1,-m}$ from which the FRI-upsampled counterpart is generated is obtained by applying the original Gaussian kernel on $I_{1,K-m}$ followed by down-scaling by a factor 2^K: $I_{1,-m} = (I_{1,K-m} * k_s) \downarrow 2^K$. In the next step, the 2D FRI-based upsampling algorithm is used to upsample $I_{1,-m}$ by a factor 2^K to obtain the corresponding FRI image $I^{FRI}_{1,K-m}$. With the FRI and bicubic upsampled image $I^{FRI}_{1,K-m}$, $I_{1,K-m}$ at hand, the DRRN can be trained with patches extracted from this image pair (step 4). After the DRRN converges, the FRI image I^{FRI}_K up-scaled from the original LR image I_0 (step 5) is then fed into the learned DRRN to get a first corrected image $I^c_{1,K}$ (step 6).

At the second stage as depicted in Fig. 2 (b), we further update the GT image using the output of the first stage $I^c_{1,K}$ and meanwhile increase the resolution level of the training image pairs. Specifically, the GT image $I_{2,K-m}$ is updated by down-scaling $I^c_{1,K}$ by a factor 0.8 using bicubic interpolation (Fig. 2 (b) step 1), in this case $m = -\log_2 0.8$, and its corresponding $I^{FRI}_{2,K-m}$ is obtained in the same way as at the first stage (step 2-3). The new training image pair is now at a scale higher than that at the first stage to gain more generalization ability and to exploit more scales. A new DRRN is then trained based on the new image pair (step 4). To gradually refine the GT image, the second stage is iterated three times by generating the GT image from the output of the previous iteration (step 5-6).

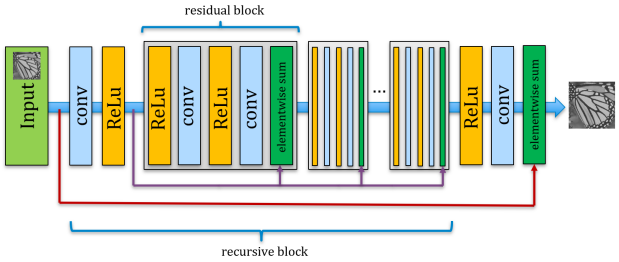

Fig. 3. The architecture of DRRN. The purple line indicates local identity branch while the red line indicates global identity branch.

C. The image-specific DRRN

The imprecision of the piece-wise smooth model of natural images will inevitably introduce artefacts in the super-resolved images. This is because the piecewise polynomial assumption will result in immediate transitions between two pixels at the edges. Inspired by the work of Ying *et al.* [4], we propose to train a DRRN in a self-supervised manner to further refine the super-resolved images as discussed in the previous section.

The DRRN is composed of one recursive block with 10 residual units and has a total depth of 22 layers as shown in Fig. 3. Inside the residual unit, each convolutional layer has 64 channels and the filter kernel is of size 3×3. The weights are shared among each residual unit. The input of the identity branch to all residual units is the output of the first convolutional layer. As a consequence, there are going to be multiple residual and identity paths between the input and the output of the network and this helps to learn highly complex features. It also helps gradient backpropagation.

We use L_2 loss with Adam optimizer to update the parameters of the network. The learning rate is set to $l = 2 \times 10^{-3}$. To enrich the dataset, we employ data augmentation by getting a random crop from I_{K-m} and I^{FRI}_{K-m} (see Fig. 2 (a)) respectively, and perform perspective transformation with a random rotation angle and shift on both patches. The network is trained stochastically (batch size of 1) over these patch pairs.

IV. Experiments and Discussions

In this section, we evaluate the performance of different SISR algorithms both numerically and visually. *Set5* [35] and *Urban100* [16] are used as test datasets. We consider up-scaling factors of 2 and 4 and compare our proposed method with state-of-the-art self-learning SISR methods, including FRESH [15], SelfEx [16] and ZSSR [25], an example-based non-deep SISR method SRF [14], and supervised DCNN, including EDSR+ [5], DRLN+ [8] and HAN+ [9]. For all self-learning methods, to make sure the comparison is fair, we replace the down-sampling kernels with the ground-truth down-sampling kernels where applicable. For non-deep SISR methods, we retrained the model with the original down-sampling kernel and B-spline functions are used in the up-sampling process. And for supervised-learning algorithms, we directly apply their pre-trained network model on our LR images.

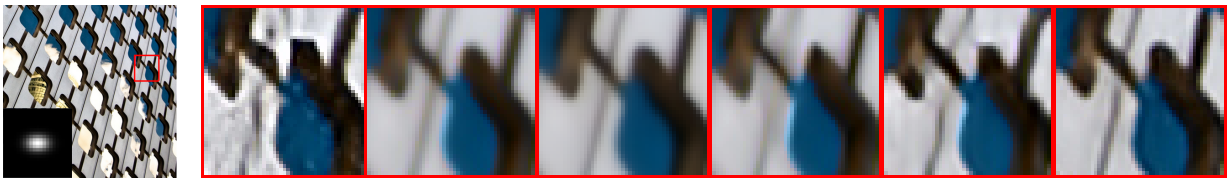

(a) GT image and anisotropic kernel | (b) FRESH [15] (19.87/0.7952) | (c) EDSR+ [5] (21.06/0.7064) | (d) HAN+ [9] (21.34/0.7221) | (e) SelfEX [16] (21.27/0.7130) | (f) ZSSR [25] (21.59/0.7234) | (g) Our (23.80/0.7951)

Fig. 4. Visual comparison on *"img041"* of *Urban100* for up-scaling factor of 4.

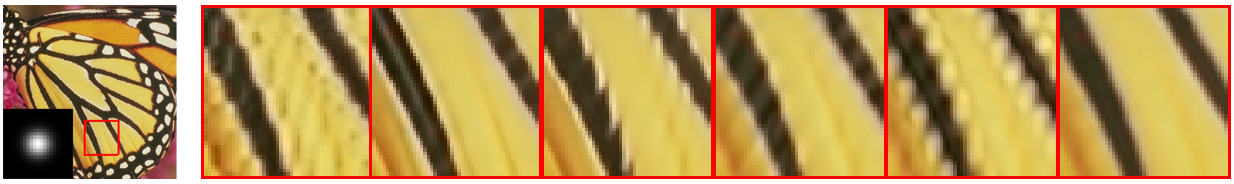

(a) GT image and isotropic kernel | (b) FRESH [15] (20.31/0.7145) | (c) EDSR+ [5] (22.52/0.8116) | (d) HAN+ [9] (22.30/0.7952) | (e) SelfEx [16] (21.95/0.7273) | (f) ZSSR [25] (21.36/0.7058) | (g) Our (24.10/0.8025)

Fig. 5. Visual comparison on *"butterfly"* of *Set5* for up-scaling factor of 4.

TABLE I
NUMERICAL COMPARISON OF AVERAGE PSNR/SSIM ON *Set5* AND *Urban100* FOR UP-SCALING FACTORS OF 2 AND 4.

		Supervised				Self-supervised			
	scale	EDSR+ [5]	DRLN+ [5]	HAN+ [9]	SRF [14]	ZSSR [25]	SelfEx [16]	FRESH [15]	Our
Set5	×2	–	–	–	34.06	–	–	30.94	**34.22**
		–	–	–	**0.9404**	–	–	0.8763	0.9377
	×4	27.69	27.30	27.32	28.96	26.85	27.30	27.04	**29.01**
		0.8131	0.8134	0.8363	0.8518	0.7997	0.8174	0.7931	**0.854**
Urban100	×2	–	–	–	28.58	–	–	25.14	**29.06**
		–	–	–	0.8820	–	–	0.7758	**0.8914**
	×4	22.74	22.56	22.58	23.55	23.06	22.60	20.77	**23.75**
		0.6889	0.7023	0.7019	0.7301	0.7242	0.6763	0.6188	**0.7580**

Table. 1 reports the average PSNR and SSIM [36]. For up-scaling factor of 2, some algorithms are not considered due to half-pixel miss alignment. The results show that our method achieves better numerical performance than the comparison SISR algorithms. Note that even if we retrain the SRF with the ground-truth down-sampling kernels using external dataset, our method still achieves better performance. This indicates the usefulness of exploiting internal recurrent information. The results also show that when the test LR images do not satisfy the conditions under which the network is trained, the pre-trained externally-supervised DCNN algorithms could barely benefit from their learned prior statistics. Even though FRESH [15] also employs FRI-upsampling algorithm, the fact that the down-sampling kernel is not exactly a scaling function deteriorates its performance drastically. Instead, we could mitigate the impact stemmed from the imprecision in approximation by leveraging self-supervised deep networks to correct artefacts. ZSSR [25] achieves comparatively good results among unsupervised algorithms on datasets with more internal repetitive patches, which is due to exploiting cross-scale internal statistics, however, for up-scaling factor 4, its performance is around 2.1 dB and 0.7 dB lower than our proposed algorithm on *Set5* and *Urban100* respectively.

Fig. 4 and Fig. 5 show two exemplar visual results using different SISR methods. Supervised DCNN results tend to be blurry since the testing condition mismatches the training condition. Self-learning methods tend to yield better results on LR images with large internal patch repetitions, but still suffer from blurring or oversharping. Our proposed method, benefiting from simultaneously exploiting the properties of FRI-based reconstruction and self-learning deep networks, can recover SR images with sharp edges and less artefacts, and avoid oversharpening on smoother image area.

V. CONCLUSIONS

We have proposed a novel SISR algorithm that leverages both the FRI sampling theory and the power of self-learning deep networks. By modelling PSFs as scaling functions, we first apply FRI upsampling algorithm to recover rich high-pass image details. Then a self-supervised DRRN is trained on patches extracted solely from the LR and FRI-upsampled image. On LR images whose down-sampling kernel can be well modeled with scaling functions, our algorithm yields state-of-the-art performance.

REFERENCES

[1] C. Dong, C. C. Loy, K. He, and X. Tang, "Image super-resolution using deep convolutional networks", *IEEE Transactions on Pattern Analysis and Machine Intelligence*, vol. 38, no. 2, pp. 295-307, 2015.

[2] J. Kim, J. K. Lee, and K. M. Lee, "Accurate image super-resolution using very deep convolutional networks", in *Proceedings of IEEE Conference on Computer Vision and Pattern Recognition*, pp. 1646-1654, 2016.

[3] J. Kim, J. K. Lee, and K. M. Lee, "Deeply-recursive convolutional network for image super-resolution", *IEEE Conference on Computer Vision and Pattern Recognition*, pp. 1637-1645, 2016.

[4] Y. Tai, J. Yang, and X. Liu, "Image super-resolution via deep recursive residual network", *IEEE Conference on Computer Vision and Pattern Recognition*, pp. 2790-2798, 2017.

[5] B. Lim, S. Son, H. Kim, S. Nah, and K. M. Lee, "Enhanced deep residual networks for single image super-resolution", in *Proceedings of IEEE Transactions on Computer Vision and Pattern Recognition Workshops*, 2017.

[6] X. Deng, R. Yang, M. Xu, and P. L. Dragotti, "Wavelet Domain Style Transfer for an Effective Perception-distortion Tradeoff in Single Image Super-Resolution", in *ICCV*, 2019.

[7] W. Sun, Z. Chen, "Learned Image Downscaling for Upscaling using Content Adaptive Resampler", in *IEEE Transactions on Image Processing*, vol. 29, pp. 4027-4040, 2020.

[8] S. Anwar and N. Barnes, "Densely Residual Laplacian Super-Resolution," in IEEE Transactions on Pattern Analysis and Machine Intelligence, 2020.

[9] Y. Zhang, K. Li, Kai Li, L. Wang, B. Zhong, and Y. Fu, "Single Image Super-Resolution via a Holistic Attention Network", ECCV 2020.

[10] Y. Zhang, K. Li, K. Li, L. Wang, B. Zhong, Y. Fu, "Image Super-Resolution Using Very Deep Residual Channel Attention Networks", ECCV, 2018.

[11] W. T. Freeman, T. R. Jone, and E. C. Pasztor, "Example-based super-resolution", *IEEE Computer Graphics and Applications*, vol. 22, no. 22, pp. 56-65, 2002.

[12] R. Timofte, V. D. Smet, and L. V. Gool, "A+: Adjusted anchored neighborhood regression for fast super-resolution", *Asian Conference on Computer Vision*, pp. 111-126, 2014.

[13] R. Zeyed, M. Elad, and M. Protter, "On single image scale-up using sparse representation", *International Conference on Curves and Surfaces*, pp. 711-730, 2010.

[14] S. Schulter, C. Leistner, and H. Bischof, "Fast and accurate image upscaling with super-resolution forests", *IEEE Conference on Computer Vision and Pattern Recognition*, pp. 3791-3799, 2015.

[15] X. Wei and P. L. Dragotti, "FRESH–FRI-based single-image super-resolution algorithm", *IEEE Transactions on Image Processing*, vol. 25, no. 8, pp. 3723-3735, 2016.

[16] J. Huang, A. Singh, and N. Ahuja, "Image super-resolution from transformed self-exemplars", *IEEE Conference on Computer Vision and Pattern Recognition*, pp. 5197-5206, 2015.

[17] J. J. Huang, W. C. Siu, and T. R. Liu, "Fast image interpolation via random forests", *IEEE Transactions on Image Processing*, vol. 24, no. 10, pp. 3232 - 3245, 2015.

[18] J. J. Huang, T. R. Liu, P. L. Dragotti, and T. Stathaki, "SRHRF+: Self-example enhanced single image super-resolution using hierarchical random forests", *IEEE Conference on Computer Vision and Pattern Recognition Workshops*, pp. 71-79, 2017.

[19] M. Bevilacqua, A. Roumy, C. Guillemot, and M.-L. A. Morel, "Single-image super-resolution via linear mapping of interpolated self-examples", *IEEE Transactions on image processing*, vol. 23, no. 12, pp. 5334-5347, 2014.

[20] N. Efrat, D. Glasner, A. Apartsin, B. Nadler, and A. Levin, "Accurate blur models vs. image priors in single image super-resolution", *IEEE International Conference on Computer Vision*, pp. 2832-2839, 2013.

[21] X. Wang, K. Yu, S. Wu, J. Gu, Y. Liu, C. Dong, Y. Qiao, and C. C. Loy, "ESRGAN: Enhanced super-resolution generative adversarial networks", *ECCV*, pp. 701-710, 2018.

[22] X. Wang, L. Xie, C. Dong, and Y. Shan, "Real-esrgan: Training real-world blind super-resolution with pure synthetic data", *arXiv preprint arXiv:2107.10833*, 2021.

[23] K. Zhang, J. Liang, L. V. Gool, and R. Timofte, "Designing a practical degradation model for deep blind image super-resolution", *IEEE Conference on International Conference on Computer Vision*, 2021.

[24] J. Liang, J Cao, G. Sun, K. Zhang, L. V. Gool, R. Timofte, "SwinIR: Image Restoration Using Swin Transformer", *IEEE International Conference on Computer Vision Workshops*, 2021.

[25] A. Schoher, N. Cohen, and M. Irani, " 'Zero-shot' super-resolution using deep internal-learning", *IEEE Conference on Computer Vision and Pattern Recognition*, pp. 3118-3126, 2018.

[26] S. Bell-Kligler, A. Shocher, M. Irani, "Blind Super-Resolution Kernel Estimation using an Internal-GAN", *NeurIPS*, 2019.

[27] C. D. Claxton and R. C. Staunton, "Measurement of the point-spread function of a noisy imaging system", *Journal of the Optical Society of America A*, vol. 25, pp. 159-170, 2008.

[28] P. L. Dragotti, M. Vetterli, and T. Blu, "Sampling moments and reconstructing signals of finite rate of innovation: Shannon meets Strang-Fix", *IEEE Transactions on Signal Processing*, vol. 55, no. 5, pp. 1741-1757, 2007.

[29] M. Unser, "Splines: A perfect fit for signal and image processing", *IEEE Signal Processing Magazine*, vol. 16, no. 6, pp. 22-38, 1999.

[30] M. Zontak and M. Irani, "Internal statistics of a single natural image", *IEEE Conference on Computer Vision and Pattern Recognition*, pp. 977-984, 2011.

[31] S. G. Mallat, "A theory for multiresolution signal decomposition: The wavelet representation", *IEEE Transactions on Pattern Analysis and Machine Intelligence*, vol. 11, no. 7, pp. 674-693, 1989.

[32] M. Vetterli and J. Kovačević, "Wavelets and subband coding", *Prentice-Hall*, 1995.

[33] A. Cohen, I. Daubechies, and J.-C. Feauveau, "Biorthogonal bases of compactly supported wavelets", *Communications on Pure and Applied Mathematics*, vol. 45, pp. 485-560, 1992.

[34] K. He, X. Zhang, S. Ren, and J. Sun, "Identity mapping in deep residual networks", *European Conference on Computer Vision*, pp. 630-645, 2016.

[35] M. Bevilacqua, A. Roumy, and M.-L. A. Morel, "Low-complexity single-image super-resolution based on nonnegative neighbor embedding", *The British Machine Vision Conference*, 2012.

[36] Z. Wang, A. C. Bovik, H. R. Sheikh, and E. P. Simoncelli, "Image quality assessment: from error visibility to structural similarity", *IEEE Transactions on Image Processing*, vol. 13, no. 4, 2004.

[37] M. Unser, A. Aldroubi, and M. Eden, "On the asymptotic convergence of B-spline wavelets to Gabor functions", *IEEE Transactions on Information Theory*, vol. 38, no. 2, pp. 864-872, 1992.

[38] Y. Wang, S. L. Lee, "Scale-space derived from B-splines", *IEEE Transactions on Pattern Analysis and Machine Learning*, vol. 20, no. 19, 1998.

[39] X. Deng, J. Huang, M. Liu and P. L. Dragotti, "U-Fresh: An Fri-Based Single Image Super Resolution Algorithm and An Application in Image Compression," *ICASSP*, pp. 1807-1811, 2018.

[40] J. W. Soh, S. Cho and N. I. Cho, "Meta-Transfer Learning for Zero-Shot Super-Resolution", CVPR, 2020.